Progress In Electromagnetics Research, Vol. 111, 433–445, 2011

MICROWAVE PROPERTIES OF A HIGH-TEMPERATURE SUPERCONDUCTOR AND FERROMAGNETIC BILAYER STRUCTURE

C.-J. Wu and Y.-L. Chen

Institute of Electro-Optical Science and Technology
National Taiwan Normal University
Taipei 11677, Taiwan, R.O.C.

Abstract—Microwave properties for a bilayer structure made of the high-temperature superconducting and the ferromagnetic materials are theoretically investigated. The properties are explored through the effective surface impedance calculated by using the enhanced two-fluid model for high-temperature superconductors together with the transmission line theory. The calculated effective surface impedance will be numerically analyzed as a function of the frequency, the temperature, and the thicknesses of the constituent layers. It is found that, for a thinner superconducting film, the effective surface resistance is a strong function of the frequency, and the effective surface reactance exhibits a peak and a dip in the frequency-domain. In the study of the effect of thickness in ferromagnetic substrate, there is a peak frequency in the surface reactance for a thinner substrate. There is also a threshold thickness for the ferromagnetic substrate such that it behaves like a bulk substrate when its thickness is larger than this threshold value. In the temperature dependence of surface reactance, the peak near critical temperature is shifted to lower temperature and broadened as the film thickness decreases.

Received 13 November 2010, Accepted 15 December 2010, Scheduled 19 December 2010
Corresponding author: Chien-Jang Wu (jasperwu@ntnu.edu.tw).

1. INTRODUCTION

It is known that the microwave surface impedance is a useful quantity in the description of the response to an electromagnetic microwave field for a superconducting material [1–10]. For a superconductor occupying the half space, $z \geq 0$, the microwave surface impedance is defined as

$$Z_s = R_s + jX_s = \frac{E_t(z=0)}{\int\limits_0^\infty J_s(z)dz}, \tag{1}$$

where the E_t $(z = 0)$ is the tangential electric field at the plane boundary of $z = 0$, and J_s is the surface current density flowing parallel to the plane boundary. In Equation (1), the real part, R_s, and the imaginary part, X_s, are called the surface resistance and surface reactance, respectively. According to the London local electrodynamics and the two-fluid model, at microwave frequencies which are well below superconducting gap frequency, expressions for the surface resistance and surface reactance read [11],

$$R_s = \frac{1}{2}\omega^2\mu_0^2\sigma_n x_n \lambda_L^3, \tag{2}$$

$$X_s = \omega\mu_0\lambda_L, \tag{3}$$

where μ_0 is the free-space permeability, ω is the angular frequency of the microwave radiation, x_n is the fraction of the normal fluid, σ_n is normal-state conductivity, and λ_L is the temperature-dependent London penetration depth. The study of surface impedance has two important aspects. The first is from the applicational viewpoint, i.e., the knowledge of R_s indicates the electromagnetic dissipation of the superconductor, which in turn determines the performance of the superconductor-based devices. The second is of fundamental importance because a basic parameter of superconductivity, the superconducting penetration length, can be extracted from the measurement of X_s according to Equation (3).

Equations (2) and (3) derived from the definition of Equation (1) indicate the microwave surface impedance of a bulk superconductor. Since Equations (2) and (3) have nothing to do with the thickness of a superconductor, it is thus known as an intrinsic surface impedance of a bulk material. However, microwave surface impedance measurements are, in reality, conducted by a layered structure where the superconducting thin film is deposited on the relevant dielectric substrate. In this case, the microwave surface impedance is commonly referred to as the effective surface impedance which can be calculated by using the impedance transform technique in the transmission line theory (TLT).

There have been many theoretical and experimental reports on the microwave effective surface impedance for the typical high-temperature superconducting system, $YBa_2Cu_3O_{7-x}$ (YBCO) [1–5, 7]. For YBCO, the relevant dielectric substrate includes lanthanum aluminate, $LaAlO_3$, magnesium oxide, MgO, and strontium titanate, $SrTiO_3$ (STO), as well. In the YBCO/STO layered structure, the temperature-dependent effective surface resistance shows an oscillating behavior because the permittivity of STO is nonlinear, i.e., it is strongly dependent on the temperature and the external applied static electric field [12, 13]. Using semiconductor Si as a substrate, the study of surface impedance of YBCO/Si has been reported recently [14]. The integration of superconductor and semiconductor is promising in low-temperature microelectronics.

In addition to the above-mentioned substrates, YBCO is often combined with some certain magnetic material to form a layered structure. Such a composite structure plays a useful and important role in exploring the fundamental and applicational issues on the superconductivity and the magnetism as well. For instance, based on the magnetic and transport properties of hybrid superconducting system, a manganite/YBCO bilayer can be used as a spintronic sensor [15]. A planar transmission line made of YBCO and magnetic yttrium iron garnet (YIG) can be employed to investigate the propagation properties of a magnetostatic surface wave [16]. A trilayer waveguide consisting of antiferromagnet, superconductor, and semiconductor is used to explore the propagation characteristics of nonlinear transverse magnetic (TM) surface wave [17, 18]. Recently, a report on the optical properties in the ferromagnet-superconductor superlattice demonstrates the occurrence of novel feature of an electromagnetic metamaterial, i.e., the negative index of refraction [19]. Moreover, the inherent spin-valve effect can be theoretically investigated in the hybrid structure of ferromagnet-superconductor-ferromagnet [20].

Motivated by the above-mentioned possible combinations of YBCO and the relevant magnetic materials, in this paper, we would like to calculate the microwave effective surface impedance for a bilayer structure made of YBCO film deposited on the ferromagnetic substrate, $La_{0.7}Sr_{0.3}MnO_3$ (LSMO). To explore the electromagnetic microwave response of YBCO, a more accurate two-fluid model called the enhanced two-fluid (ETF) model will be used in our calculation [21]. The effective surface impedance will be investigated as a function of the frequency, the temperature and the static applied magnetic field.

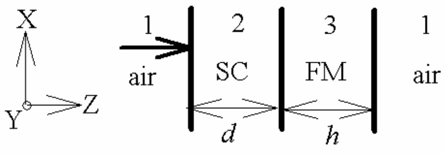

Figure 1. A superconductor-ferromagnet bilayer structure for the calculation of effective surface impedance. The electromagnetic microwave radiation is incident normally from the left region 1 at the plane boundary of $z = 0$. The thicknesses of superconductor (SC) and the ferromagnetic (FM) are d and h, respectively.

2. BASIC EQUATIONS

Let us consider an SC/FM bilayer structure shown in Figure 1, in which the region 1 is free space, the superconductor (SC = YBCO) with a thickness of d is in region 2, and the region 3 is occupied by the ferromagnetic (FM, which is taken to be LSMO in this study) with a thickness of h. An electromagnetic monochromatic plane wave (with x-polarized electric field) propagating in z direction is normally incident on the plane boundary of air/SC, $z = 0$. Meanwhile, the FM layer is under an external static magnetic field H_0 applied parallel to x direction such that its saturation magnetization M is also parallel to H_0.

To model the electrodynamics of a high-quality YBCO film, we shall adopt the enhanced two-fluid (ETF) model reported by Vendik et al. [21]. According to this model, the relative permittivity of YBCO at $T < T_c$ can be expressed as

$$\varepsilon_{r2}(\omega, T) = -\frac{j}{\omega\varepsilon_0}[\sigma_{2,r}(T) - j\sigma_{2,i}(\omega, T)], \tag{4}$$

where $\sigma_{2,r}(T)$ and $\sigma_{2,i}(\omega, T)$ are respectively the real and imaginary parts of the superconducting complex conductivity given by

$$\sigma_{2,r}(T) = \sigma_n\{(T/T_c)^{\gamma-1} + \alpha[1 - (T/T_c)^{\gamma}]\}, \tag{5}$$

$$\sigma_{2,i}(\omega, T) = \frac{1}{\omega\mu_0\lambda_0^2[1 - (T/T_c)^{\gamma}]^{-1}}. \tag{6}$$

Here, σ_n is the normal-state conductivity of YBCO at $T = T_c$ and λ_0 is the London penetration depth at $T = 0\,\mathrm{K}$. In addition, α and γ are the empirical parameters. All these parameters, $T_c = 90\,\mathrm{K}$, $\alpha = 6.5$, $\gamma = 2$, $\lambda_0 = 200\,\mathrm{nm}$, and $\sigma_n = 10^6\,\mathrm{S/m}$ for YBCO will be used in our next calculation. It is worth mentioning that $\gamma = 4$ is commonly taken for the conventional superconductors. For high-temperature cuprates such as the high quality YBCO thin-film, γ is experimentally shown to be not equal to four, but around two. With the permittivity in Equation (4), the associated wave number of YBCO is given by

$$k_2 = \omega\sqrt{\mu_0\varepsilon_0\varepsilon_{r2}} = k_0\sqrt{\varepsilon_{r2}}, \tag{7}$$

where $k_0 = \omega\sqrt{\mu_0\varepsilon_0}$ is the free-space wave number. In addition, the intrinsic impedance of YBCO is

$$Z_2 = \sqrt{\frac{\mu_0}{\varepsilon_0\varepsilon_{r2}}} = \frac{Z_0}{\sqrt{\varepsilon_{r2}}}, \tag{8}$$

where $Z_0 = \sqrt{\mu_0/\varepsilon_0} = 120\pi = 377\,\Omega$ is the intrinsic impedance of free space.

As for the FM-LSMO layer, the complex-valued relative permittivity is expressed as [22]

$$\varepsilon_{r3} = \varepsilon'_{r3} - j\frac{\sigma_3}{\varepsilon_0\omega} \tag{9}$$

where ε'_{r3} is the real part, and σ_3 is the normal conductivity of ferromagnetic material. As seen in Figure 2 of [23], the measured normal conductivity σ_3 is a function of the temperature. According to this figure, at $T < T_c$, σ_3 can be approximated as the following relation, i.e.,

$$\sigma_3(T) = \frac{10^5}{1.39\times10^{-3}T + 0.33324}. \tag{10}$$

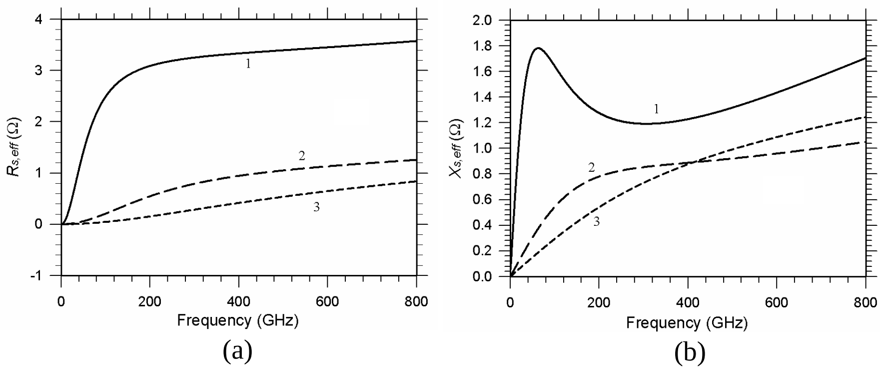

Figure 2. The calculated frequency-dependent (a) effective surface resistance $R_{s,\mathit{eff}}$ and (b) effective surface reactance $X_{s,\mathit{eff}}$ at $T = 77\,\mathrm{K}$, $\mu_0H_0 = 100\,\mathrm{mT}$, and $h = 1\,\mu\mathrm{m}$ for three different thicknesses of YBCO film $d = 0.1\lambda_0$, λ_0, $10\lambda_0$ (curves 1–3, respectively).

On the other hand, the relative permeability of FM-LSMO is given by

$$\mu_{r3} = \mu - \frac{\mu_a^2}{\mu}, \tag{11}$$

where

$$\mu_a = \frac{\omega\omega_M}{\omega_H^2 - \omega^2}, \tag{12}$$

and

$$\mu = 1 + \frac{\omega_M\omega_H}{\omega_H^2 - \omega^2}, \tag{13}$$

where $\omega_M = \mu_0\gamma M$, $\omega_H = \mu_0\gamma H_0 + j\frac{\mu_0\alpha_1\omega}{2\pi}$, γ is the gyromagnetic ratio and α_1 is the coefficient for the damping term. For LSMO, the saturation magnetization M is also a function of the temperature. The measured M can be seen in Figure 2 of [23]. Using this temperature-dependent plot in M, we can approximate it as the following relation,

$$M(T) = \frac{-5.25 \times 10^{-4}T + 0.759}{4\pi}, \tag{14}$$

for $T < T_c$. The associated wave number of LSMO is

$$k_3 = \omega\sqrt{\mu_0\varepsilon_0\mu_{r3}\varepsilon_{r3}} = k_0\sqrt{\mu_{r3}\varepsilon_{r3}}, \tag{15}$$

In addition, the intrinsic impedance is

$$Z_3 = \sqrt{\frac{\mu_0\mu_{r3}}{\varepsilon_0\varepsilon_{r3}}} = Z_0\sqrt{\frac{\mu_{r3}}{\varepsilon_{r3}}}. \tag{16}$$

The effective surface impedance $Z_{s,\mathit{eff}}$ for the structure in Figure 1 can be calculated by making use of the impedance transformation technique in TLT. First, the impedance at the interface of SC/FM, $z = d$, is expressed as

$$Z_{\mathrm{SC/FM}}(\omega, h) = Z_3\frac{Z_1 + Z_3\tanh(jk_3h)}{Z_3 + Z_1\tanh(jk_3h)}, \tag{17}$$

where the impedance Z_1 is equal to Z_0. Next, the effective surface impedance at the incident plane boundary of air/SC, $z = 0$, is given by

$$\begin{aligned} Z_{s,\mathit{eff}}(\omega, T, d, h) &= R_{s,\mathit{eff}}(\omega, T, d, h) + jX_{s,\mathit{eff}}(\omega, T, d, h) \\ &= Z_2\frac{Z_{\mathrm{SC/FM}} + Z_2\tanh(jk_2d)}{Z_2 + Z_{\mathrm{SC/FM}}\tanh(jk_2d)}. \end{aligned} \tag{18}$$

With $Z_{\mathrm{SC/FM}}(\omega, h)$ given in Equation (17), it is seen that $Z_{s,\mathit{eff}}(\omega, T, d, h)$ expressed in Equation (18) incorporates all possible material parameters, including the intrinsic properties such as the permittivities and permeabilities, and the extrinsic properties like the thicknesses of the constituent layers.

3. NUMERICAL RESULTS AND DISCUSSION

In Figure 2, we plot (a) the effective surface resistance $R_{s,eff}$ and (b) the effective surface reactance $X_{s,eff}$ as a function of the frequency for three different thicknesses of YBCO, $d = 0.1\lambda_0$, λ_0, and $10\lambda_0$ (corresponding to curves 1–3, respectively) at $T = 77\,\mathrm{K}$ and $\mu_0 H_0 = 100\,\mathrm{mT}$. The material parameters for the ferromagnetic LSMO are $\gamma = 28 \times 10^9 (T-s)^{-1}$, $\alpha_1 = 0.01$, and $h = 1\,\mu\mathrm{m}$. It is seen that for a thin YBCO film, $d = 0.1\lambda_0$ (curve 1), the surface resistance is larger than those for $d = \lambda_0$ and $10\lambda_0$ (curves 2–3). In addition, $R_{s,eff}$ increases as the frequency increases for $d = 0.1\lambda_0$, and it increases pronouncedly below 160 GHz and then slowly increases as frequency increases. As for the effective surface reactance $X_{s,eff}$, it is seen from (b) that, for $d = 0.1\lambda_0$, there exists a peak near 60 GHz and a broad dip around 300 GHz. In addition, the curves 2 and 3 intersect near 400 GHz. For SC with thickness $d = \lambda_0$ or $10\lambda_0$ both $R_{s,eff}$ and $X_{s,eff}$ monotonically increases as a function of the frequency.

Next, let us study the effect due to the change of the thickness in LSMO layer. In Figure 3, we plot (a) the effective surface resistance $R_{s,eff}$ and (b) the effective surface reactance $X_{s,eff}$ as a function of the frequency for four LSMO thicknesses, $h = 0.1, 1, 10$ and $100\,\mu\mathrm{m}$ (corresponding to the curves 1–4, respectively). Here, $T = 77\,\mathrm{K}$, $\mu_0 H_0 = 100\,\mathrm{mT}$ and $d = 200\,\mathrm{nm}$ are taken. It is seen that for a thin LSMO film, $h = 0.1\,\mu\mathrm{m}$ (curve 1), the surface resistance is larger than those for thicker ones (curves 2–4) at frequencies higher than

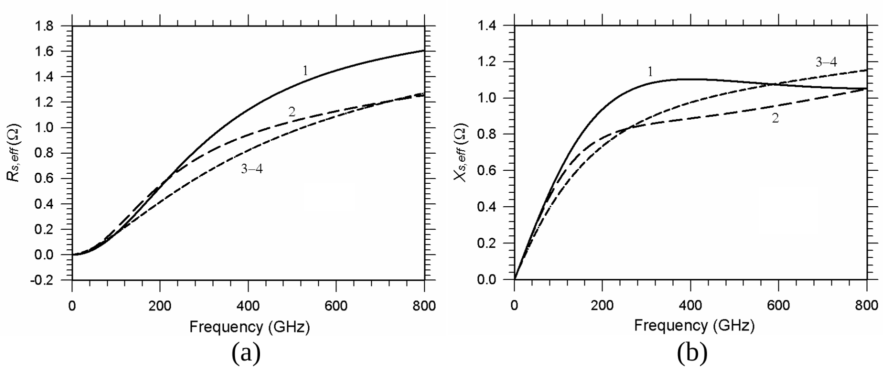

Figure 3. The calculated frequency-dependent (a) effective surface resistance $R_{s,eff}$ and (b) effective surface reactance $X_{s,eff}$ at $T = 77\,\mathrm{K}$, $\mu_0 H_0 = 100\,\mathrm{mT}$, and $d = 200\,\mathrm{nm}$ for four different thicknesses of LSMO film $h = 0.1, 1, 10, 100\,\mu\mathrm{m}$ (curves 1–4, respectively).

200 GHz. In addition, $R_{s,eff}$ increases as the frequency increases for all curves 1–4. However, if the LSMO thickness is larger than or equal to 10 μm, the curves of the frequency-dependent $R_{s,eff}$ coincide, as seen in curves 3 and 4. The same feature is also seen in $X_{s,eff}$. This enables us to define a threshold thickness of LSMO, hth = 10 μm such that the LSMO effectively behaves as a bulk substrate when $h \geq h$th. Moreover, the effective surface reactance $X_{s,eff}$ shown in (b), for $h = 0.1$ μm, there exists a maximum point near 300 GHz. This maximum point is then smeared out when the LSMO thickness increases.

The temperature-dependent effective surface resistance $R_{s,eff}$ and effective surface reactance $X_{s,eff}$ for three YBCO thicknesses, $d = 0.1\lambda_0$, λ_0, and $10\lambda_0$ (curves 1–3) are plotted in Figures 4(a) and (b), respectively. Here $f = 100$ GHz, $\mu_0 H_0 = 100$ mT, and $h = 1$ μm. It is seen that for a thin YBCO film, $d = 0.1\lambda_0$ (curve 1), the effective surface resistance is larger than those for $d > 0.1\lambda_0$ (curves 2–3). As for the effective surface reactance $X_{s,eff}$, the usual peak at temperature below T_c is also seen for the magnetic substrate. The peak height is enhanced and broadened when the thickness of YBCO film is small. In addition, the position of peak is shifted to the temperature away from T_c. The peak just below T_c mainly arises from the combined effects of the temperature-dependent London penetration depth and the film size effect. According to Equation (6), the London penetration depth is given by

$$\lambda_L(T) = \lambda_0[1 - (T/T_c)^{\gamma}]^{-1/2}. \tag{19}$$

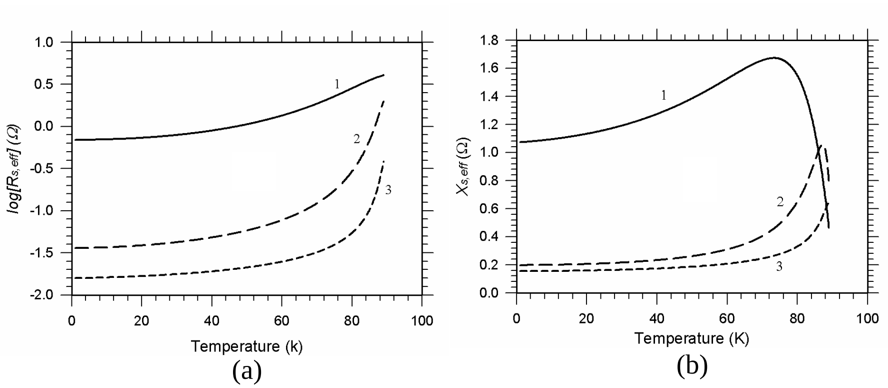

Figure 4. The calculated temperature-dependent (a) effective surface resistance $R_{s,eff}$ and (b) effective surface reactance $X_{s,eff}$ at $f = 100$ GHz, $\mu_0 H_0 = 100$ mT, and $h = 1$ μm for three different thicknesses of YBCO film $d = 0.1\lambda_0$, λ_0, $10\lambda_0$ (curves 1–3, respectively).

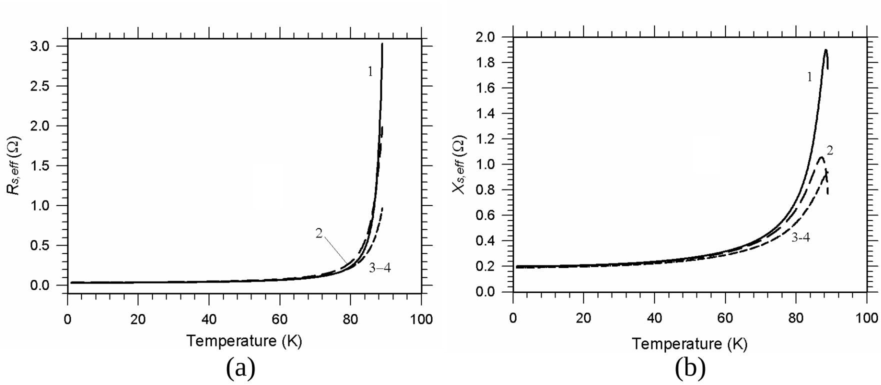

Figure 5. The calculated temperature-dependent (a) effective surface resistance $R_{s,eff}$ and (b) effective surface reactance $X_{s,eff}$ at $f = 100\,\text{GHz}$, $\mu_0 H_0 = 100\,\text{mT}$, and $d = 200\,\text{nm}$ for four different thicknesses of LSMO film, $h = 0.1, 1, 10, 100\,\mu\text{m}$ (curves 1–4, respectively).

For a bulk superconductor, Equation (3) indicates that the surface reactance will, in principle, go to infinite as T approaches T_c because $\lambda_L(T \to T_c) \to \infty$ based on Equation (19). It is thus no peak can be seen in the bulk one. However, if the bulk material is replaced by the film, the effect of London penetration depth will be compensated by the film size effect, causing the large value in $X_{s,eff}$ to lower down and produce a peak, as shown in the curves 1 and 2 of Figure 4(b). It can be seen that this compensating effect is more pronounced for a thinner film. For a film with thickness equal to and larger than $10\lambda_0$ (as curve 3) this peak will not emerge, indicating that the size effect is much weaker than effect of the penetration depth.

In Figure 5 we plot (a) the effective surface resistance $R_{s,eff}$ and (b) the effective surface reactance $X_{s,eff}$ as a function of the temperature for four LSMO thicknesses, $h = 0.1, 1, 10$ and $100\,\mu\text{m}$ (curves 1–4, respectively) at $f = 100\,\text{GHz}$, $\mu_0 H_0 = 100\,\text{mT}$, and $d = 200\,\text{nm}$. It is seen that there is no apparent distinction in $R_{s,eff}$ for curves 1–4 at $T < 80\,\text{K}$. The insignificant change reveals that the thickness effect coming from LSMO is not so important as YBCO. As for $X_{s,eff}$, we see that the LSMO thickness has a strong influence in the peak height below T_c. However, the positions of peak in curves 1 and 2 remain nearly unchanged, as illustrated in Figure 4(b).

Figure 6 depicts the effective surface resistance $R_{s,eff}$ as a function of the temperature at three different static magnetic fields, $\mu_0 H_0 = 100, 500, 1000\,\text{mT}$ (curves 1–3, respectively), where $f = 100\,\text{GHz}$, $h = 1\,\mu\text{m}$, and $d = 200\,\text{nm}$ are used. The result shows that the effective surface resistance is nearly not affected by applying the different

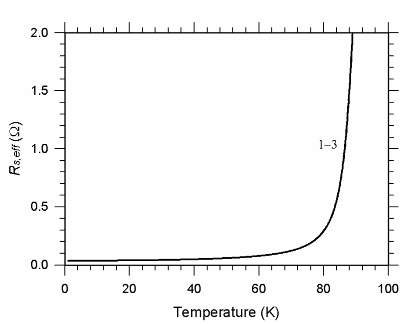

Figure 6. The calculated temperature-dependent (a) effective surface resistance $R_{s,\mathit{eff}}$ for three different $\mu_0 H_0 = 100\,\mathrm{mT}$, $500\,\mathrm{mT}$, $1\mathrm{T}$ (curves 1–3, respectively) at $f = 100\,\mathrm{GHz}$, $h = 1\,\mu\mathrm{m}$, and $d = 200\,\mathrm{nm}$.

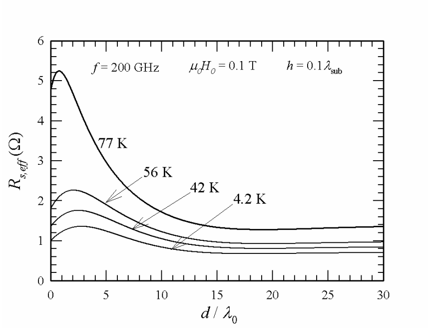

Figure 7. The calculated effective surface resistance $R_{s,\mathit{eff}}$ as a function of the thickness of the superconducting thin film for three different temperatures, 77, 56, 42, and 4.2 K, respectively.

static magnetic field. It indicates the static magnetic field acting on the LSMO layer has effectively no influence on the effective surface resistance for the YBCO/LSMO bilayer structure.

In Figure 7, we plot $R_{s,\mathit{eff}}$ as a function of the thickness of the superconducting thin film d at 200 GHz for different temperatures of $T = 77, 56, 42$, and 4.2 K, respectively. Here, we take $\mu_0 H_0 = \mathrm{mT}$ and LSMO thickness $h = 0.01\lambda_{\mathrm{sub}}$, where $\lambda_{\mathrm{sub}} = 2\pi/|k_3| = 2.242\,\mu\mathrm{m}$. At 77 K, there is a peak at $d/\lambda_0 = 1$, which can be characterized as a threshold thickness for the property of $R_{s,\mathit{eff}}$. For thickness d less than this threshold value, $R_{s,\mathit{eff}}$ increases as d increases, and then decreases as d increases. The threshold thickness is moved to a higher value as the temperature decreases.

We have so far numerically analyzed the microwave surface impedance of a bilayer made of a high-T_c superconductor and a ferromagnet. Indeed, such a bilayer has attracted much attention over the last decade. Nevertheless, theoretical and experimental reports on the microwave surface impedance of this structure are still few. Thus, the present numerical results can motivate the experimentalists to extract information of the microwave surface impedance based on the different experimental techniques such as the cavity resonator method [12], the magnetotransmission and magnetoreflection measurements [24], and the magneto-optical measurement [25].

4. CONCLUSION

The effective surface impedance of a layered structure made of YBCO and LSMO has been theoretically calculated and investigated. Based on the numerical results, some conclusions can be drawn.

1. The effect of thickness on the surface impedance coming from YBCO layer is more salient than LSMO layer. A pronounced variation in the surface impedance can be seen for YBCO thickness less than λ_0.
2. In this bilayer structure, no substantial effect from the variation of the static magnetic field on the surface impedance can be seen.
3. There is a threshold thickness for the LSMO layer. The LSMO film can be effectively regarded as a bulk substrate when its film thickness is larger than or equal to this threshold thickness.
4. There is also a threshold thickness for the superconducting thin film that characterizes two different thickness-dependent behaviors. This threshold thickness increases as the temperature decreases.

ACKNOWLEDGMENT

C.-J. Wu acknowledges the financial support from the National Science Council of the Republic of China (Taiwan) under Contract No. NSC-97-2112-M-003-013-MY3.

REFERENCES

1. Trunin, M. R., "Temperature dependence of microwave surface impedance in high-T_c single crystals," *J. Supercond.*, Vol. 11, 381–408, 1998.
2. Newman, N. and W. G. Lyons, "High-temperature superconducting microwave devices," *J. Supercond.*, Vol. 6, 119–216, 1993.
3. Gallop, J., "Microwave applications of high-temperature superconductors," *Supercond. Sci. Technol.*, Vol. 10, 120–141, 1997.
4. Porch, A. and M. J. Lancaster, "Introduction to the special issue of the proceedings of the 9th symposium on high temperature superconductors in high frequency fields," *J. Supercond. Novel Magn.*, Vol. 20, 1, 2007.
5. Lancaster, M. J., *Passive Microwave Device Applications of High-temperature Superconductors*, University of Birmingham, 1997.

6. Wu, C.-J., C.-M. Fu, and T.-J. Yang, "Microwave surface impedance of a nearly ferroelectric superconductor," *Progress In Electromagnetics Research*, Vol. 73, 39–47, 2007.
7. Wu, C.-J., Y.-L. Chen, and Y.-S. Tsai, "Effective surface impedance for a superconductor-semiconductor superlattic at mid-infrared frequency," *Journal of Electromagnetic Waves and Applications*, Vol. 23, Nos. 11–12, 1441–1453, 2009.
8. Wu, C.-J., "Thickness-dependent effective surface resistances of nearly ferroelectric superconductors," *Phys. Lett. A*, Vol. 364, 163–166, 2007.
9. Wu, C.-J., "Microwave response of a nearly ferroelectric superconductor," *J. Appl. Phys.*, Vol. 100, 063908-1-6, 2006.
10. Wu, C.-J., "Effective microwave surface impedance of a type-II superconducting thin film in the parallel magnetic field," *J. Appl. Phys.*, Vol. 93, 3450–3456, 2003.
11. Duzer, T. V. and C. W. Turner, *Principle of Superconductive Devices and Circuits*, Elsevier, New York, 1981.
12. Klein, N., H. Chaloupka, G. Muller, S. Orbach, H. Piel, B. Roas, L. Schultz, U. Klein, and M. Peiniger, "The effective microwave surface impedance of high T_c thin films," *J. Appl. Phys.*, Vol. 67, 6940–6945, 1990.
13. Wu, C.-J., "Tunable microwave characteristics of a superconducting planar transmission line by using a nonlinear dielectric thin film," *J. Appl. Phys.*, Vol. 87, 493–497, 2000.
14. Pompeo, N., R. Marcon, and E. Silva, "Substrate contribution to the surface impedance of HTS films on Si," *J. Supercond. Novel Magn.*, Vol. 19, 611–615, 2006.
15. Lin, J. G., D. Hsu, A. Mani, and T. G. Kumary, "Utilizing the superconducting bilayer as a spintronic sensor," *Progress In Electromagnetics Research Symposium Abstracts*, 370, Moscow, Russia, August 18–21, 2009.
16. Tsutsumi, M., T. Fukusako, and S. Yoshida, "Propgation characteristics of the magnetostatic surface wave in YBCO-YIG film-layered structure," *IEEE Trans. Microwave Theory Technology*, Vol. 44, 1410–1415, 1996.
17. Hamada, M. S., M. M. Shabat, M. M. Abd Elaal, and D. Jager, "Characteristics of TM surface waves in a nonlinear antiferromagnet-semiconductor-superconductor waveguide structure," *J. Supercond.*, Vol. 16, 443–447, 2003.
18. Wu, C.-J., "Field solution of nonlinear magnetic surface wave for a planar superconductor-antiferromagnet transmission line,"

J. Appl. Phys., Vol. 104, 063909–063909-5, 2008.

19. Pimenov, A., A. Loidl, P. Przyslupski, and B. Dabrowski, "Negative refraction in ferromagnet-superconductor superlattices," *Phys. Rev. Lett.*, Vol. 95, 247009, 2005.
20. Faure, M., A. I. Buzdin, and D. Gusakova, "On the theory of ferromagnet/superconductor heterostructures," *Physica C*, Vol. 454, 61–69, 2007.
21. Vendik, O. G., I. B. Vendik, and D. I. Kaparkov, "Empirical model of the microwave properties of high-temperature superconductors," *IEEE Trans. Microwave Theory Technology*, Vol. 46, 469–478, 1998.
22. Nurgaliev, T., "Numerical investigation of the surface impedance of ferromagnetic manganite thin films," *J. Magn. Magn. Mat.*, Vol. 320, 304–311, 2008.
23. Nurgaliev, T., "Modeling of the microwave characteristics of layered superconductor/ferromagnetic structures," *Physica C*, Vol. 468, 912–919, 2008.
24. Moser, E. K., W. J. Tomasch, M. W. Coffey, C. L. Pettiette-Hall, and S. M. Schwarzbek, "Microwave properties of $YBa_2Cu_3O_{7-\delta}$ films at 35 GHz from magnetotransmission and megnetoreflection measurements," *Phys. Rev. B*, Vol. 49, 4199–4208, 1994.
25. Gozzelino, L., F. Laviano, P. Przyslupski, A. Tsarou, A. Wisniewski, D. Botta, R. Gerbaldo, and G. Ghigo, "Quantitative magneto-optical analysis of twinned $YBa_2Cu_3O_{7-\delta}$/LaSrMnO bilayers," *Supercond. Sci. Technol.*, Vol. 19, 50–54, 2006.